Jaehde Ulrich (Orcid ID: 0000-0002-2493-7370)

Population pharmacokinetic analyses of regorafenib and capecitabine in patients with locally advanced rectal cancer (SAKK 41/16 RECAP)

Running title: PK modeling of regorafenib and capecitabine

Eduard Schmulenson (1), Cédric Bovet (2), Regula Theurillat (2), Laurent Arthur Decosterd (3), Carlo R. Largiadèr (2), Jean-Christophe Prost (2), Chantal Csajka (4), Daniela Bärtschi (5), Matthias Guckenberger (6), Roger von Moos (7), Sara Bastian (7)§, Markus Joerger (8)§, Ulrich Jaehde (1)§*

(1) Institute of Pharmacy, Department of Clinical Pharmacy, University of Bonn, Bonn, Germany
(2) Department of Clinical Chemistry, Inselspital, Bern University Hospital and University of Bern, Bern, Switzerland
(3) Laboratory of Clinical Pharmacology, Lausanne University Hospital and University of Lausanne, Lausanne, Switzerland
(4) Clinical Pharmaceutical Sciences, Lausanne University, Lausanne, Switzerland
(5) SAKK Coordinating Center, Bern, Switzerland
(6) Department of Radiation Oncology, University Hospital Zurich, University of Zurich, Zurich, Switzerland
(7) Cantonal Hospital Graubünden, Chur, Switzerland
(8) Department of Medical Oncology and Hematology, Cantonal Hospital St. Gallen, St. Gallen, Switzerland

§shared senior authorship

***Corresponding author**

Prof. Dr. Ulrich Jaehde
Institute of Pharmacy
University of Bonn
An der Immenburg 4
53121 Bonn
Germany

Phone: +49 228 73 5252
Fax: +49 228 73 9757
Email: u.jaehde@uni-bonn.de
ORCID: 0000-0002-2493-7370

This article has been accepted for publication and undergone full peer review but has not been through the copyediting, typesetting, pagination and proofreading process which may lead to differences between this version and the Version of Record. Please cite this article as doi: 10.1111/bcp.15461

Principal Investigator statement: The authors confirm that the Principal Investigator for this paper is Sara Bastian and that she had direct clinical responsibility for patients.

Word count: 4170/4000

Number of tables and figures: 3 tables, 5 figures

Number of references: 57

Abstract

Aim: Locally advanced rectal cancer (LARC) is an area of unmet medical need with one third of patients dying from their disease. With response to neoadjuvant chemo-radiotherapy being a major prognostic factor, trial SAKK 41/16 assessed potential benefits of adding regorafenib to capecitabine-amplified neoadjuvant radiotherapy in LARC patients.

Methods: Patients received regorafenib at three dose levels (40/80/120 mg once daily) combined with capecitabine 825 mg/m² bidaily and local radiotherapy. We developed population pharmacokinetic models from plasma concentrations of capecitabine and its metabolites 5'-deoxy-5-fluorocytidine and 5'-deoxy-5-fluorouridine as well as regorafenib and its metabolites M-2 and M-5 as implemented into SAKK 41/16 to assess potential drug-drug interactions (DDI). After establishing parent-metabolite base models, drug exposure parameters were tested as covariates within the respective models to investigate for potential DDI. Simulation analyses were conducted to quantify their impact.

Results: Plasma concentrations of capecitabine, regorafenib and metabolites were characterized by one- and two compartment models and absorption was described by parallel first- and zero-order processes and transit compartments, respectively. Apparent capecitabine clearance was 286 L/h (relative standard error [RSE] 14.9%, interindividual variability [IIV] 40.1%) and was reduced by regorafenib cumulative area under the plasma-

concentration curve (median reduction of 45.6%) as exponential covariate (estimate -4.10×10^{-4}, RSE 17.8%). Apparent regorafenib clearance was 1.94 L/h (RSE 12.1%, IIV 38.1%). Simulation analyses revealed significantly negative associations between capecitabine clearance and regorafenib exposure.

Conclusions: This work informs the clinical development of regorafenib and capecitabine combination treatment and underlines the importance to study potential DDI with new anticancer drug combinations.

What is already known about this subject:

- Patients with locally advanced rectal cancer suffer from frequent locoregional and systemic relapse.
- The addition of the tyrosine kinase inhibitor regorafenib to capecitabine-augmented local radiotherapy is a promising strategy to improve pathological response rates.

What this study adds:

- Our population pharmacokinetic models show a negative impact of regorafenib cumulative area under the plasma-concentration curve on capecitabine clearance.
- The drug-drug interaction between regorafenib and capecitabine seems to be of negligible clinical relevance.

Keywords

Capecitabine, Regorafenib, Rectal Cancer, Population Pharmacokinetics, Drug-Drug Interaction

Introduction

Colorectal cancer (CRC) is the third most common cause of cancer cases worldwide and ranks second in cancer deaths [1]. While the overall incidence of CRC declined in many high-income countries in recent years, CRC incidence in adults younger than 50 years increased substantially [1, 2], mainly driven by rising cases of rectal cancer [3]. Rectal cancer comprises about one third of the total colorectal cancer cases [4, 5]. Neoadjuvant chemo-radiotherapy followed by potentially curative surgery is standard of care in patients with locally advanced rectal cancer (LARC). Alternatively, the watchful waiting strategy after complete pathological response of neoadjuvant chemo-radiotherapy is another approach in LARC patients, requiring intensification of therapy [6]. Response to neoadjuvant chemo-radiotherapy is an important independent prognostic factor [7], still the rate of complete pathological response is only 10-25% [8, 9], and one third of patients with LARC relapse after chemo-radiotherapy and surgery [10]. Recent studies added tyrosine kinase inhibitors (TKI) such as sorafenib [11] or cediranib [12] to capecitabine-based chemo-radiotherapy in LARC to improve clinical outcome. Trial SAKK 41/16 added the second-generation multi-TKI regorafenib to capecitabine-based chemo-radiotherapy, and this trial included a pharmaco-translational part with extensive pharmacokinetic (PK) analysis of both anticancer drugs to assess for potential drug-drug interactions (DDI).

Neoadjuvant chemo-radiation with capecitabine has been shown to be tolerated both alone and in combination with irinotecan [13] or oxaliplatin [14]. Optimal dosing of oral capecitabine in combination with radiotherapy has been established at 825 mg/m² bidaily given throughout the course of radiotherapy [15]. Regorafenib is an oral multi-TKI with broad activity, including inhibition of angiogenesis (VEGFR1-3, TIE2), impact on the tumor

microenvironment (PDGFR-β, FGFR) and oncogenesis (KIT, PDGFR, and RET) [16]. Regorafenib has been approved as monotherapy in patients with advanced CRC, hepatocellular carcinoma and gastrointestinal stromal tumors at a daily dose of 160 mg. Regorafenib has a bioavailability of 69% [17] and is metabolized to active metabolites M-2 (regorafenib N-oxide) and M-5 (N-desmethyl-regorafenib) by CYP3A4 and UGT1A9 [18]. Mean elimination half-life of M-2 and M-5 is 24 and 51-64 hours, respectively. Excretion of regorafenib is mainly via feces (50%) and less via the kidneys (19%) [17]. Capecitabine is sequentially converted to 5'-deoxy-5-fluorocytidine (DFCR) by hepatic carboxylesterase and to 5'-deoxy-5-fluorouridine (DFUR) by cytidine deaminase. The intermediate DFUR is converted to fluorouracil by the enzyme thymidine phosphorylase in the final activating step. Capecitabine is a known inhibitor of CYP2C9, but potential DDI based on CYP2C9 are not expected as regorafenib is not metabolized by this enzyme. However, as regorafenib and capecitabine have overlapping toxicity, including palmar-plantar erythrodysesthesia and diarrhea [16, 19], it is important to identify potential DDI.

The aim of this study was to implement population PK models of regorafenib, capecitabine and their metabolites in LARC patients, and to investigate potential interactions between both drugs.

Methods

Patients and data

This open-label, multi-center, non-randomized phase IB trial explored the recommended dose of and pathological response to regorafenib when added to capecitabine-augmented neoadjuvant chemo-radiotherapy in patients with AJCC stage II/III rectal cancer (mrT3/4 N0,

mrTx N1-2 cM0). SAKK 41/16 recruited 25 patients from six Swiss sites between March 2017 and April 2021. The trial includes a dose-escalation part and an expansion cohort after establishing the recommended phase-2 dose. All patients were tested for mutations of the dihydropyrimidine dehydrogenase gene (*DPYD*), and patients harboring one of four dysfunctional *DPYD* mutations (*DPYD* c.1679T>G [rsrs55886062], c.1905+1G>A [rsrs3918290], c.2846A>T [rs67376798], c.1129-5923C>G [rs75017182]) were excluded from SAKK 41/16 [20, 21]. Furthermore, only patients between 18 and 75 years with adequate renal (creatinine clearance >50 mL/min) and hepatic function (markers such as bilirubin, alanine/aspartate aminotransferase ≤1.5× the upper limit of normal) were included. The study was conducted according to the Declaration of Helsinki and patients provided written informed consent before participation. The study protocol was approved by the respective regulatory authorities and registered under clinicaltrials.gov number NCT02910843.

PK data from 12 patients enrolled into the dose-escalation cohort were used for the development of the population PK models as no blood samples were obtained from patients belonging to the expansion cohort. Patients received oral capecitabine 825 mg/m² bidaily on days 1 to 38. Regorafenib was administered at three dose levels (40, 80 and 120 mg) once daily on days 1 to 14 and days 22 to 35. Local radiotherapy was given in all patients at 1.8 Gy per day in 28 fractions (5.6 weeks) for a total dose of 50.4 Gy. Patients underwent rectal cancer surgery 6-12 weeks (+/- 1 week) after completion of chemo-radiotherapy. Plasma samples for analysis of regorafenib, capecitabine and their metabolites were collected on day 1 (0.5, 1, 2, 3, 4 and 6 h after dosing) followed by post-dose sampling on days 2, 4, 8, 15, 22, 29 and 36. PK sampling after day 1 occurred at the time of the patient's appointment and was not bound to a specific time-point. Patient characteristics are outlined in Tab. 1.

Quantification of drug concentrations

Plasma concentrations of regorafenib and its active metabolites M-2 and M-5 were quantified using a validated liquid chromatography coupled to tandem mass spectrometry assay as previously described [22]. Plasma concentrations of capecitabine and its metabolites DFCR and DFUR were quantified using a second validated assay by liquid chromatography coupled to tandem mass spectrometry between 0.5 and 10 µg/mL plasma. This assay was validated according to the US Food and Drug Administration and C62-A of the Clinical and Laboratory Standards Institute Guidelines [23, 24]. Validation parameters fulfilled the acceptance criteria of these guidelines. The results of the validation parameters are shown in Tables S1-1 to S1-4 of the Supporting Information (SI). The lower limit of quantification for the assay was 0.25 µg/mL. Reference standards for capecitabine and DFCR/DFUR were obtained from Santa Cruz Biotechnology, Inc. (Heidelberg, Germany) and TCI Deutschland GmbH (Eschborn, Germany), respectively. The isotope-labeled internal standards capecitabine $^{2}H_{11}$, DFCR $^{13}C^{15}N_2$, DFUR $^{13}C^{15}N_2$ were obtained from Toronto Research Chemicals (Toronto, Canada). Stock solutions and dilutions were prepared in acetonitrile:water 1:1 (v/v). Calibrators (0.5-10 µg/mL) and quality controls (1.5, 5 and 9 µg/mL) were prepared in pooled plasma (Dunn Labortechnik GmbH). After thawing the plasma samples at 4°C, 10 µL acetonitrile:water 1:1 (v/v) (for calibrators and QCs the corresponding standard dilution) and 140 µL acetonitril:ethanol 1:1 (v/v) containing the internal standards were added to 50 µL of plasma in a 96 well plate. The plate was sealed and shaked at 1000 rpm and room temperature for 5 minutes. After centrifugation (4000 relative centrifugal force, room temperature, 20 minutes), 20 µL of the supernatant were diluted with 300 µL of water in a new 96 well plate with a pipetting robot (Liquid Handling Station LHS, Brand, Germany). Finally, the plate was sealed and shaked at

room temperature at 1000 rpm for 5 minutes. 3 µl of the extracted samples were analyzed by reversed-phase chromatography (Acquity UPLC HSS T3 column, 2.1 x 50 mm, 1.7 µM, Waters) on a triple quadrupole mass spectrometer (Xevo TQ-S, Waters) coupled to an UPLC Acquity I-Class system (Waters). Capecitabine, DFCR, and DFUR were separated at 0.4 mL/min with a gradient using water (A) and methanol (B) acidified with 0.05% (v/v) formic acid as mobile phases (0.0-1.0 min, 1% B; 1.0-4.5 min, 1-95% B; holded for 1 min, then switched back to 1% B and equilibrated from 5.1-7.0 min). The source offset and transition parameters were optimized for each analyte. The raw data were processed with TargetLynx available in the MassLynx software (version 4.1, Waters).

Population pharmacokinetic models

Population PK analysis of the concentration-time data of regorafenib and capecitabine was performed using the nonlinear mixed-effect modeling software NONMEM version 7.5 (double precision, level 1.1). [25]. NONMEM uses a maximum likelihood criterion to simultaneously estimate population values of fixed-effects variables (e.g., drug clearance) and values of random-effects variables (e.g., interindividual, interoccasion, and residual variability). The likelihood-ratio test was used to discriminate between nested models. The inclusion of an extra parameter required a statistically significant reduction ($p < 0.05$) of the objective function value (OFV) provided by NONMEM®. Non-nested models were compared by the Akaike Information Criterion (AIC). Implemented scripts in PsN (version 5.0.0) [26, 27] were used for model development and R (version 4.1.0) [28] was used for graphical purposes. Piraña (version 2.9.7) [29] served as front interface.

Structural model development of the capecitabine-metabolite model

In order to describe the absorption process of capecitabine, different absorption models were tested (first-, zero-order absorption, combined zero- and first-order absorption, transit absorption models). Additionally, we tested absorption models as described previously for oral capecitabine [30–32], as the corresponding plasma concentrations supported a fast initial absorption phase (Fig. S2-1 of the SI).

The population PK parent-metabolite model was developed in three sequential steps. After establishing the parent drug model, its structural parameters were fixed and the subsequent metabolites were included in a stepwise fashion. Eventually, all parameters were estimated simultaneously [34]. One- and two-compartment models were evaluated for the description of the plasma concentration-time course of capecitabine and its metabolites. Since the bioavailability F of capecitabine and the fractions converted to the metabolites were structurally unidentifiable, model parameters were estimated relative to these values (e.g. clearance/F). Overall, plasma concentrations below the lower limit of quantification (0.25 µg/mL for capecitabine and metabolites, 0.02 µg/mL for regorafenib and metabolites) were included for model development [35].

Structural model development of the regorafenib-metabolite model

Model development steps for regorafenib, M-2 and M-5 were identical to the procedure for capecitabine and its metabolites. Besides one- and two-compartment models, three-compartment models were investigated for the description of the plasma concentrations of

the respective compounds as well. In addition, different enterohepatic circulation (EHC) models as described previously [36–38] were additionally investigated.

Statistical model development

Population PK parameters were assumed to be log-normally distributed and inter-individual variability (IIV) was implemented as an exponential function [39]. We tested different error models (additive, proportional, combined additive/proportional) to describe residual PK variability [39]. Inter-occasion variability (IOV) was explored on clearance and absorption parameters as well [39].

Covariate analysis

The resulting capecitabine- and regorafenib-metabolite base models were used to generate drug exposure parameters. In a covariate analysis, concentrations over time and cumulative area under the curve (AUC) over time of regorafenib, M-2 and M-5 were tested on the clearance of capecitabine and its metabolites, and the same PK parameters were also tested on the clearance of regorafenib and its metabolites. Laboratory parameters were preselected as covariates if they were associated with a Common Terminology Criteria for Adverse Events (CTCAE) grade >0 [40] in at least 15% of total measurements. Covariates were implemented into the model in a stepwise forward inclusion and backward elimination approach using the scm script implemented in PsN [26, 27]. In the forward selection process, covariates which led to a significant decrease of the OFV ($p < 0.05$) were kept for further evaluation. The final forward model was re-evaluated by backward elimination of each covariate with a significance level of $p < 0.01$. If a covariate was still significant in this step, the plausibility of its effect as well as a successful model convergence was assessed and eventually kept in the

model. Exponential and linear parameter-covariate relations were tested for continuous and categorical covariates, respectively.

For covariate analysis, the above-mentioned drug exposure parameters as well as demographic data (sex, age, weight, height, body surface area, body mass index), bilirubin and hemoglobin concentration were preselected. Even though bilirubin concentration exhibited a rather narrow range at baseline (Tab. 1) it was nevertheless included as the number of CTCAE grades >0 increased during the course of therapy (concentration range 2 – 32 µmol/L).

Model evaluation

The precision of model parameter estimates defined as the relative standard error (RSE) assisted in model evaluation. Models which converged with a successful covariance step, were considered for further analysis. In order to assess the model fit, goodness-of-fit plots [41] as well as prediction-corrected visual predictive checks (pcVPC) were used. For the development of a pcVPC 5^{th}, 50^{th} and 95^{th} percentiles with the respective 95% confidence intervals (CI) were generated from 1000 simulated datasets based on the observed dataset and superimposed by the observed plasma concentrations over time. Both simulated and observed plasma concentrations were normalized with respect to the median prediction [42]. pcVPC were constructed in R using a modified code originally provided by the PMX Solutions website [43]. In addition, model robustness as well as precision and bias of parameter estimates were evaluated by non-parametric bootstrap analysis without stratification. Median and 95% CI of parameter estimates were derived from 1000 replicate datasets obtained from sampling individuals from the original dataset with replacement.

Simulation study

The final population PK and covariate models were forwarded to extensive simulation studies. Here, the impact of potential covariates including drug interactions on the PK of capecitabine, regorafenib or their metabolites were analyzed. The PK model of capecitabine containing the identified exposure parameter of regorafenib as covariate was therefore simulated. Values of this regorafenib drug exposure parameter were previously generated via simulation of its PK model. For days 1, 8, 15, 22, 29 and 36, geometric mean drug clearances of capecitabine were calculated, along with their respective 95% CI.

Results

Model building

For the development of the population PK parent-metabolite models, 86 capecitabine, 126 DFCR and 132 DFUR plasma concentration measurements were included as well as 151 regorafenib, 141 M-2 and 113 M-5 plasma concentration measurements.

Capecitabine and metabolites

The observed plasma concentration-time course of capecitabine, DFCR, and DFUR were best described by a one-compartment model (Fig. 1). Model parameter estimates and bootstrap results are presented in Tab. 2. Residual variability was modeled using a proportional error model. Implementation of IOV was not successful due to run errors. In order to describe capecitabine absorption, a parallel first- and zero-order absorption model was most appropriate (Tab. S3-1 of the SI). The relatively slow first-order absorption process of capecitabine in combination with a rapid elimination indicated a flip-flop PK for capecitabine.

Estimating the volume of distribution of the metabolite DFUR resulted in values close to the boundary of zero. This finding in combination with a similar decay of DFCR and DFUR plasma concentrations (Fig. S1-2 and S1-3 of the SI) indicated a flip-flop PK for DFUR as well [32]. Therefore, only an elimination rate constant for DFUR (k_e, DFUR) was estimated and an IIV term on this rate constant was implemented.

The covariate analysis for the capecitabine-metabolite model is presented in Tab. S3-2 of the SI. The final model included regorafenib cumulative AUC as a covariate on capecitabine clearance, which led to a stable model along with a significant drop in OFV compared to the base model (-33.918, $p < 0.00001$).

The identified exponential covariate led to a reduction of capecitabine clearance estimates (Eq.1):

$$CL_{Cap} = CL_{Cap,pop} \times e^{(-\theta \times AUC_{Reg,cum})} \times e^{\eta_{i,CL_{Cap,pop}}} \quad \text{Eq. 1}$$

CL_{Cap} denotes the individual capecitabine clearance estimate, $CL_{Cap,pop}$ the population estimate of capecitabine clearance, θ is the covariate effect estimate, $AUC_{Reg,cum}$ is the cumulative AUC over time of regorafenib and $\eta_{iCLCap,pop}$ represents the IIV term for the capecitabine population clearance of the i^{th} individual with a mean of 0 and a variance of ω^2. The median reduction of capecitabine clearance was 45.6% at day 36 (derived from a median regorafenib cumulative AUC from day 0 to 36 of 1458.5 µmol×h/L).

Bootstrap estimates were in accordance with estimates from the final model. The models correctly described the observed data as depicted in the pcVPC (Fig. 2) and in the goodness-of-fit plots (Fig. S3-1 – S3-3 of the SI). The pcVPC additionally indicated flip-flop PK for capecitabine, DFCR and DFUR due to a slow absorption or formation process.

Regorafenib and metabolites

Plasma concentrations of regorafenib, M-2 and M-5 were best described by two-compartment models with a proportional error model. Due to a non-significant reduction in OFV, IOV was not incorporated. A summary of the model parameter estimates including the bootstrap results is presented in Tab. 3. A transit compartment model with Erlang distribution as previously described by Rosseau et al. and Lindauer et al. [44, 45] was the most suitable in order to describe regorafenib absorption (Tab. S3-3 of the SI). Mean absorption time (MAT) was estimated and a transfer rate constant (k_{tr}) between these compartments was calculated as follows (Eq. 2):

$$k_{tr} = \frac{Number\ of\ transit\ compartments}{MAT} \qquad \text{Eq. 2}$$

The formation of M-2 and M-5 is outlined in Fig. 3. M-2 metabolism was best described by presystemic formation occurring from the first transit compartment of regorafenib. A series of transit compartments was chosen for the description of M-2 absorption as well. Since PK data after direct administration of M-2 and M-5 were not available and the conversion percentages were unknown, the volumes of distribution of M-2 and M-5 could not be estimated. Therefore, it was assumed that their volumes of distributions as well as the intercompartmental clearances were the same as that of regorafenib. IIV terms on the clearances of all three compounds, the shared volume of distribution and the mean absorption time of regorafenib were successfully included. Available plasma concentration data of regorafenib and its metabolites did not support the implementation of EHC models.

Covariate analyses of regorafenib-metabolite base models are presented in Tab. S3-4 of the SI. None of the identified covariates remained in the final model. The pcVPC (Fig. 4) as well as

the goodness-of-fit plots (Fig. S3-4 – S3-6 of the SI) showed an adequate description of the observed data although the depiction of the observed data versus the population predictions of M-2 and M-5 revealed a tendency towards an underprediction of higher plasma concentration values.

Simulation study

The impact of regorafenib cumulative AUC on capecitabine clearance was submitted to simulation analysis as described above. The final regorafenib-metabolite model was used to simulate 1000 subjects for each regorafenib dose level (40/80/120 mg once daily) until day 36. The treatment schedule equaled the schedule from the study (2 weeks of treatment, 7-day break, another 2 weeks of treatment). A capecitabine dose of 1500 mg bidaily (corresponding to 825 mg/m² bidaily) was chosen and simulation was subsequently performed including the regorafenib cumulative AUC as covariate for the same time period. In addition, 1000 patients without regorafenib were simulated. The simulation results are depicted in Fig. 5 (from 792 – 864 hours) and Fig. S4-1 of the SI (total simulation time period). Calculated capecitabine clearance values are presented for various time points in Tab. S4-1 of the SI. A higher regorafenib dose and subsequent cumulative AUC was associated with a lower capecitabine clearance (Tab. S4-1) and hence reduced capecitabine metabolism to active metabolites. Whereas capecitabine clearance was comparable between regorafenib dose levels on day one, the impact of regorafenib on capecitabine clearance increased with increasing cumulative regorafenib exposure (Tab. S4-1). With decreasing capecitabine clearance, formation of DFCR and DFUR was expected to decrease likewise. Like for capecitabine, CIs of the concentration-time curves of DFCR and DFUR overlapped in the beginning as well whereas they became more diverged with increasing cumulative

regorafenib exposure. However, the differences in metabolite exposure were negligible between the different regorafenib dose levels including simulations with 0 mg regorafenib. The respective plots are presented in Fig. 5 as well as Fig. S4-2 and S4-3 of the SI.

Discussion

This is the first study evaluating the addition of the multi-TKI regorafenib to capecitabine-augmented local radiotherapy in LARC patients. We successfully developed population PK and covariate parent-metabolite models of regorafenib and capecitabine in patients of trial SAKK 41/16 (RECAP). The description of capecitabine absorption by parallel first- and zero-order processes differed from the absorption models of published capecitabine models in which parallel first-order [33], transit compartments [32] or first-order absorption with lag time [30, 31] were established. In fact, capecitabine absorption is highly variable due to e.g. double peaks [33], the impact of age [31], food [46] or alterations in the gastrointestinal tract including potential gastrectomy e.g. in patients with gastro-esophageal cancer [32]. One possible explanation for the identification of a dual absorption process may be the reflection of different absorption sites, namely the small intestine and the stomach [33, 46]. The slow first-order absorption process as well as comparatively slower metabolite formations were presumably responsible for the occurrence of flip-flop PK for capecitabine, DFCR, and DFUR in our model. This was also indicated by biphasic declines of the concentration-time curves despite using one-compartment models [47]. It should however be noted that the patients' first observations were almost exclusively those with the highest plasma concentrations. An additional sample could be drawn between 0 and 0.5 h, e.g. 15 minutes after dose intake as observed in the model of Jacobs et al. [32] to gain more certainty about capecitabine absorption. The establishment of one-compartment models for capecitabine, DFCR and DFUR

was in accordance with several published population PK models [30, 31, 33]. Additionally, the identified flip-flop PK of DFUR could also be observed in the model of Jacobs et al. [32].

The population PK model structure and parameters of the regorafenib-metabolite model were similar to the published model of Keunecke et al. [38]. However, in our model the formation of M-5 from M-2 was established whereas Keunecke et al. assumed that M-5 is directly formed by regorafenib [38]. The proposed metabolic pathway of Gerisch et al. indicated that M-5 is indeed formed by M-2 [48] and our population PK model did not allow to distinguish between both proposed pathways (Tab. S3-3 of the SI). The implementation of covariates was not successful as well since the inclusion of additional parameters led to model instabilities presumably due to overparameterization. The inclusion of identified covariates from the study of Keunecke et al. [38] (sex on clearance of regorafenib, M-2 and M-5, respectively, as well as BMI on regorafenib clearance) led to estimated covariate parameters with large RSE (≥ 58%) and a non-significant drop in OFV compared to the base model (-6.052, p=0.20). Furthermore, the establishment of an EHC could not be supported by the underlying data of this study. Besides a presumed overparameterization of the model the sampling time of regorafenib and its metabolites should be adjusted in order to account for the identification of EHC-caused concentration peaks. Secondary and tertiary peaks were found to be at about 6 to 8 as well as 24 hours after dose intake [18], hence additional sampling of regorafenib and its metabolites should be considered as in this trial the last sample was drawn at 6 hours.

The covariate analysis in this study revealed a significant negative influence of regorafenib cumulative AUC over time on the formation of capecitabine active metabolites. Already one week after regorafenib intake, capecitabine clearance values were significantly reduced depending on regorafenib dose levels (Tab. 4-1). This should lead to a reduced formation of

its metabolites DFCR, DFUR as well as fluorouracil which is finally converted to active metabolites. However, DFCR and DFUR exposure remained unaffected by the reduced capecitabine clearance (Fig. S4-2 and S4-3) which translates to an unaffected exposure of fluorouracil. Accordingly, we assume a negligible clinical relevance of this DDI since capecitabine-associated adverse events are mainly attributed to its metabolites [49]. However, fluorouracil was not quantified in this study since its formation occurs intracellularly and thus, it exhibits very low plasma concentrations after capecitabine administration. A possible explanation for the identified DDI could be the inhibition of the ATP-binding cassette (ABC) transporters P-glycoprotein (Pgp) or breast cancer resistance protein (BCRP) by regorafenib [50, 51] since there have been hints that capecitabine might be a substrate for ABC transporters [52–54]. However, a clinical study with regorafenib and the Pgp substrate digoxin as well as the BCRP substrate rosuvastatin showed no influence on digoxin PK but on rosuvastatin exposure by regorafenib [51]. In addition, similar effects on capecitabine exposure were observed in two clinical trials in which capecitabine was administered in combination with sorafenib which is the defluorinated form of regorafenib. Both studies reported moderately increased capecitabine AUC while co-administering sorafenib compared to control groups with capecitabine monotherapy [55, 56]. From published population PK models of capecitabine, bilirubin concentration as a linear covariate on capecitabine clearance was tested [30] but resulted in a failure of the covariance step. Since only patients with adequate hepatic and renal function (see “Methods” section) were included in this study, covariate analysis of elimination parameters for all compounds was impeded as the respective laboratory parameters exhibited a rather narrow range. It should be noted that our identified covariate effect should be carefully interpreted due to the small number of patients in this analysis. Furthermore, regorafenib was administered in lower doses than the

approved dose of 160 mg daily. Therefore, the impact of the usual daily dose of regorafenib could not be evaluated in our study. In order to assess the clinical relevance of our finding, a future double-arm study which investigates patients under capecitabine monotherapy and patients under the combination of capecitabine and regorafenib should be conducted in a larger number of study participants. Intracellular concentrations of active metabolites of fluorouracil such as 5-fluorouridine 5'-triphosphate as predictor for capecitabine toxicity [57] could be additionally quantified.

In conclusion, the developed population PK models suggest a negligible effect of regorafenib cumulative AUC on the metabolic activation of capecitabine. Our models may serve as a basis for future DDI studies in patients under therapy with both oral anticancer drugs.

Conflict of interest disclosures

All authors declare that they have no conflicts of interest that are relevant to the content of this manuscript.

Funding/support

The trial was supported by Bayer and research agreements with the following institutions: Swiss State Secretariat for Education, Research and Innovation (SERI), Swiss Cancer Research Foundation (SCS) and Swiss Cancer League (SCL).

Data availability statement

The modeling codes are provided in the Electronic Supplementary Material. Data are available from the Swiss Group for Clinical Cancer Research (SAKK) upon reasonable request.

Ethics approval statement

The study was conducted according to the Declaration of Helsinki and was approved by the respective Swiss regulatory authorities.

Patient consent statement

Patients provided written informed consent before participation.

Clinical trial registration

This trial was registered under clinicaltrials.gov number NCT02910843.

Author contribution statement

Designed research: CRL, CC, DB, RvM, SB, MJ

Performed research: ES, CB, RT, LAD, CRL, J-CP, MG, RvM, SB, MJ

Analyzed data: ES, MJ, UJ

Wrote or contributed to the writing of the manuscript: ES, CB, RT, CRL, J-CP, DB, MG, RvM, SB, MJ, UJ

Supporting Information

S1 – Assay validation results

S2 – Observed plasma concentration-time profiles

S3 – Model development

S4 – Simulation study

S5 – Model codes

References

[1] Sung H, Ferlay J, Siegel RL, et al. Global Cancer Statistics 2020: GLOBOCAN Estimates of Incidence and Mortality Worldwide for 36 Cancers in 185 Countries. CA Cancer J Clin 2021; 71: 209–249.

[2] Araghi M, Soerjomataram I, Bardot A, et al. Changes in colorectal cancer incidence in seven high-income countries: a population-based study. Lancet Gastroenterol Hepatol 2019; 4: 511–518.

[3] Saad El Din K, Loree JM, Sayre EC, et al. Trends in the epidemiology of young-onset colorectal cancer: a worldwide systematic review. BMC Cancer 2020; 20: 288.

[4] Glynne-Jones R, Wyrwicz L, Tiret E, et al. Rectal cancer: ESMO Clinical Practice Guidelines for diagnosis, treatment and follow-up. Ann Oncol 2017; 28: iv22-iv40.

[5] Siegel RL, Miller KD, Goding Sauer A, et al. Colorectal cancer statistics, 2020. CA Cancer J Clin 2020; 70: 145–164.

[6] López-Campos F, Martín-Martín M, Fornell-Pérez R, et al. Watch and wait approach in rectal cancer: Current controversies and future directions. World J Gastroenterol 2020; 26: 4218–4239.

[7] Karagkounis G, Thai L, Mace AG, et al. Prognostic Implications of Pathological Response to Neoadjuvant Chemoradiation in Pathologic Stage III Rectal Cancer. Ann Surg 2019; 269: 1117–1123.

[8] Gérard J-P, Azria D, Gourgou-Bourgade S, et al. Comparison of two neoadjuvant chemoradiotherapy regimens for locally advanced rectal cancer: results of the phase III trial ACCORD 12/0405-Prodige 2. J Clin Oncol 2010; 28: 1638–1644.

[9] Park J, Yoon SM, Yu CS, et al. Randomized phase 3 trial comparing preoperative and postoperative chemoradiotherapy with capecitabine for locally advanced rectal cancer. Cancer 2011; 117: 3703–3712.

[10] Bosset J-F, Collette L, Calais G, et al. Chemotherapy with preoperative radiotherapy in rectal cancer. N Engl J Med 2006; 355: 1114–1123.

[11] von Moos R, Koeberle D, Schacher S, et al. Neoadjuvant radiotherapy combined with capecitabine and sorafenib in patients with advanced KRAS-mutated rectal cancer: A phase I/II trial (SAKK 41/08). Eur J Cancer 2018; 89: 82–89.

[12] Marti FEM, Jayson GC, Manoharan P, et al. Novel phase I trial design to evaluate the addition of cediranib or selumetinib to preoperative chemoradiotherapy for locally advanced rectal cancer: the DREAMtherapy trial. Eur J Cancer 2019; 117: 48–59.

[13] Willeke F, Horisberger K, Kraus-Tiefenbacher U, et al. A phase II study of capecitabine and irinotecan in combination with concurrent pelvic radiotherapy (CapIri-RT) as neoadjuvant treatment of locally advanced rectal cancer. Br J Cancer 2007; 96: 912–917.

[14] Koeberle D, Burkhard R, Moos R von, et al. Phase II study of capecitabine and oxaliplatin given prior to and concurrently with preoperative pelvic radiotherapy in patients with locally advanced rectal cancer. Br J Cancer 2008; 98: 1204–1209.

[15] Krishnan S, Janjan NA, Skibber JM, et al. Phase II study of capecitabine (Xeloda) and concomitant boost radiotherapy in patients with locally advanced rectal cancer. Int J Radiat Oncol Biol Phys 2006; 66: 762–771.

[16] Strumberg D, Schultheis B. Regorafenib for cancer. Expert Opin Investig Drugs 2012; 21: 879–889.

[17] Solimando DA, Waddell JA. Drug monographs: bosutinib and regorafenib. Hosp Pharm 2013; 48: 190–194.

[18] Mross K, Frost A, Steinbild S, et al. A phase I dose-escalation study of regorafenib (BAY 73-4506), an inhibitor of oncogenic, angiogenic, and stromal kinases, in patients with advanced solid tumors. Clin Cancer Res 2012; 18: 2658–2667.

[19] Saif MW, Katirtzoglou NA, Syrigos KN. Capecitabine: an overview of the side effects and their management. Anticancer Drugs 2008; 19: 447–464.

[20] Hamzic S, Aebi S, Joerger M, et al. Fluoropyrimidine chemotherapy: recommendations for DPYD genotyping and therapeutic drug monitoring of the Swiss Group of Pharmacogenomics and Personalised Therapy. Swiss Med Wkly 2020; 150: w20375.

[21] Amstutz U, Henricks LM, Offer SM, et al. Clinical Pharmacogenetics Implementation Consortium (CPIC) Guideline for Dihydropyrimidine Dehydrogenase Genotype and Fluoropyrimidine Dosing: 2017 Update. Clin Pharmacol Ther 2018; 103: 210–216.

[22] Cardoso E, Mercier T, Wagner AD, et al. Quantification of the next-generation oral anti-tumor drugs dabrafenib, trametinib, vemurafenib, cobimetinib, pazopanib, regorafenib and two metabolites in human plasma by liquid chromatography-tandem mass spectrometry. J Chromatogr B Analyt Technol Biomed Life Sci 2018; 1083: 124–136.

[23] U.S. Food and Drug Administration. Bioanalytical Method Validation. Guidance for Industry; 2018.

[24] CLSI. Liquid Chromatography-Mass Spectrometry Methods; Approved Guidelines. CLSI document C62-A. Wayne, PA: Clinical and Laboratory Standard Institute; 2014.

[25] Bauer RJ. NONMEM Users Guide. Gaithersburg, MD, USA: Icon Development Solutions; 2021.

[26] Lindbom L, Pihlgren P, Jonsson EN, et al. PsN-Toolkit--a collection of computer intensive statistical methods for non-linear mixed effect modeling using NONMEM. Comput Methods Programs Biomed 2005; 79: 241–257.

[27] Lindbom L, Ribbing J, Jonsson EN. Perl-speaks-NONMEM (PsN)--a Perl module for NONMEM related programming. Comput Methods Programs Biomed 2004; 75: 85–94.

[28] R Core Team. R: A language and environment for statistical computing. R Foundation for Statistical Computing, Vienna, Austria. Available at: http://www.R-project.org/. Accessed 22 Dec 2021.

[29] Keizer RJ, Karlsson MO, Hooker A. Modeling and Simulation Workbench for NONMEM: Tutorial on Pirana, PsN, and Xpose. CPT Pharmacometrics Syst Pharmacol 2013; 2: e50.

[30] Urien S, Rezaí K, Lokiec F. Pharmacokinetic modelling of 5-FU production from capecitabine--a population study in 40 adult patients with metastatic cancer. J Pharmacokinet Pharmacodyn 2005; 32: 817–833.

[31] Daher Abdi Z, Lavau-Denes S, Prémaud A, et al. Pharmacokinetics and exposure-effect relationships of capecitabine in elderly patients with breast or colorectal cancer. Cancer Chemother Pharmacol 2014; 73: 1285–1293.

[32] Jacobs BAW, Deenen MJ, Joerger M, et al. Pharmacokinetics of Capecitabine and Four Metabolites in a Heterogeneous Population of Cancer Patients: A Comprehensive Analysis. CPT Pharmacometrics Syst Pharmacol 2019; 8: 940–950.

[33] Lunar N, Etienne-Grimaldi M-C, Macaire P, et al. Population pharmacokinetic and pharmacodynamic modeling of capecitabine and its metabolites in breast cancer patients. Cancer Chemother Pharmacol 2021; 87: 229–239.

[34] Stroh M, Hutmacher MM, Pang J, et al. Simultaneous pharmacokinetic model for rolofylline and both M1-trans and M1-cis metabolites. AAPS J 2013; 15: 498–504.

[35] Keizer RJ, Jansen RS, Rosing H, et al. Incorporation of concentration data below the limit of quantification in population pharmacokinetic analyses. Pharmacol Res Perspect 2015; 3: e00131.

[36] Jain L, Woo S, Gardner ER, et al. Population pharmacokinetic analysis of sorafenib in patients with solid tumours. Br J Clin Pharmacol 2011; 72: 294–305.

[37] NMusers (NONMEM UsersNet Archive). Adaptation of multiple-dose enterohepatic circulation model suggested by Luann Phillips (after Stuart Beal) 2002. Available at: https://cognigen.com/nonmem/nm/98may312002.html. Accessed 22 Dec 2021.

[38] Keunecke A, Hoefman S, Drenth H-J, et al. Population pharmacokinetics of regorafenib in solid tumours: Exposure in clinical practice considering enterohepatic circulation and food intake. Br J Clin Pharmacol 2020; 86: 2362–2376.

[39] Mould DR, Upton RN. Basic concepts in population modeling, simulation, and model-based drug development-part 2: introduction to pharmacokinetic modeling methods. CPT Pharmacometrics Syst Pharmacol 2013; 2: e38.

[40] National Cancer Institute. Common terminology criteria for adverse events. Available at: https://ctep.cancer.gov. Accessed 20 Apr 2022.

[41] Nguyen THT, Mouksassi M-S, Holford N, et al. Model Evaluation of Continuous Data Pharmacometric Models: Metrics and Graphics. CPT Pharmacometrics Syst Pharmacol 2017; 6: 87–109.

[42] Bergstrand M, Hooker AC, Wallin JE, et al. Prediction-corrected visual predictive checks for diagnosing nonlinear mixed-effects models. AAPS J 2011; 13: 143–151.

[43] PMX Solutions. A step-by-step guide to prediction corrected visual predictive checks (VPC) of NONMEM models. Available at: https://www.pmxsolutions.com/2018/09/21/a-step-by-step-guide-to-prediction-corrected-visual-predictive-checks-vpc-of-nonmem-models/. Accessed 22 Dec 2021.

[44] Lindauer A, Siepmann T, Oertel R, et al. Pharmacokinetic/pharmacodynamic modelling of venlafaxine: pupillary light reflex as a test system for noradrenergic effects. Clin Pharmacokinet 2008; 47: 721–731.

[45] Rousseau A, Léger F, Le Meur Y, et al. Population pharmacokinetic modeling of oral cyclosporin using NONMEM: comparison of absorption pharmacokinetic models and design of a Bayesian estimator. Ther Drug Monit 2004; 26: 23–30.

[46] Reigner B, Verweij J, Dirix L, et al. Effect of food on the pharmacokinetics of capecitabine and its metabolites following oral administration in cancer patients. Clin Cancer Res 1998; 4: 941–948.

[47] Neyens M, Crauwels HM, Perez-Ruixo JJ, et al. Population pharmacokinetics of the rilpivirine long-acting formulation after intramuscular dosing in healthy subjects and people living with HIV. J Antimicrob Chemother 2021; 76: 3255–3262.

[48] Gerisch M, Hafner F-T, Lang D, et al. Mass balance, metabolic disposition, and pharmacokinetics of a single oral dose of regorafenib in healthy human subjects. Cancer Chemother Pharmacol 2017; 81: 195–206.

[49] Ma WW, Saif MW, El-Rayes BF, et al. Emergency use of uridine triacetate for the prevention and treatment of life-threatening 5-fluorouracil and capecitabine toxicity. Cancer 2017; 123: 345–356.

[50] Wang Y-J, Zhang Y-K, Zhang G-N, et al. Regorafenib overcomes chemotherapeutic multidrug resistance mediated by ABCB1 transporter in colorectal cancer: In vitro and in vivo study. Cancer Letters 2017; 396: 145–154.

[51] Strumberg D, Al-Batran S-E, Takacs I, et al. A phase I study to determine the effect of regorafenib (REG) on the pharmacokinetics (PK) of substrates of P-glycoprotein (P-gp; digoxin) and breast cancer resistant protein (BCRP; rosuvastatin) in patients with advanced solid tumors. Ann Oncol 2016; 27: vi156.

[52] Zhang J, Zhang L, Yan Y, et al. Are capecitabine and the active metabolite 5-Fu CNS penetrable to treat breast cancer brain metastasis? Drug Metab Dispos 2015; 43: 411–417.

[53] Lou Y, Wang Q, Zheng J, et al. Possible Pathways of Capecitabine-Induced Hand-Foot Syndrome. Chem Res Toxicol 2016; 29: 1591–1601.

[54] Varma A, Mathaiyan J, Shewade D, et al. Influence of ABCB-1, ERCC-1 and ERCC-2 gene polymorphisms on response to capecitabine and oxaliplatin (CAPOX) treatment in colorectal cancer (CRC) patients of South India. J Clin Pharm Ther 2020; 45: 617–627.

[55] Awada A, Gil T, Whenham N, et al. Safety and pharmacokinetics of sorafenib combined with capecitabine in patients with advanced solid tumors: results of a phase 1 trial. J Clin Pharmacol 2011; 51: 1674–1684.

[56] Infante JR, Jones SF, Bendell JC, et al. A drug interaction study evaluating the pharmacokinetics and toxicity of sorafenib in combination with capecitabine. Cancer Chemother Pharmacol 2012; 69: 137–144.

[57] Janssen JM, Jacobs BAW, Roosendaal J, et al. Population Pharmacokinetics of Intracellular 5-Fluorouridine 5'-Triphosphate and its Relationship with Hand-and-Foot Syndrome in Patients Treated with Capecitabine. AAPS J 2021; 23: 23.

Tab. 1 Summary of patient characteristics at baseline (N=12)

Characteristic	***n* or median (range)**
Number of males/females	7/5
Number of patients with regorafenib dose of 40/80/120 mg	3/6/3
AJCC tumor staging	
Tumor stage (T1/T2/T3)	0/0/12
Nodal status (N0/N1/N2/Nx)	1/4/6/1
Metastases (M0/M1)	12/0
Age (years)	57 (48 – 75)
Weight (kg)	71.7 (55.9 – 96.0)
Body surface area (m^2)	1.86 (1.59 – 2.16)
Body mass index (kg/m^2)	24.4 (20.4 – 33.2)
Bilirubin concentration (µmol/L)	6 (2 – 14)
Alanine aminotransferase (U/L)	16 (10 – 34)
Aspartate aminotransferase (U/L)	20 (13 – 30)
Hemoglobin concentration (g/L)	138 (127 – 157)
Absolute neutrophil count ($10^3/\mu L$)	4.76 (4.03 – 7.98)
Creatinine clearance (mL/min)	98 (63 – 118)

Tab. 2 Parameter estimates of the capecitabine-metabolite model

Parameter	Estimate (relative standard error, %)	Shrinkage [%]	Bootstrap median (95% confidence intervals)
CL_{Cap}/F [L/h]	286 (14.9)		296 (173 – 418)
V_{Cap}/F [L]	179 (17.8)		187 (101 – 273)
k_a [1/h]	0.0714 (23.2)		0.0828 (0.0387 – 0.336)
Duration zero-order absorption [h]	0.250 (2.5)		0.336 (0.0910 – 0.658)
Fraction of the first-order absorption process [%]	21.4 (11.8)		20.2 (13.0 – 36.1)
CL_{DFCR}/F [L/h]	123 (10.5)		122 (93.5 – 151)
V_{DFCR}/F [L]	71.9 (17.5)		67.2 (37.3 – 96.7)
$k_{e,\ DFUR}$ [1/h]	99.2 (9.6)		100 (82.4 – 125)
Regorafenib cumulative AUC effect on CL_{Cap}/F	-4.10×10^{-4} (17.8)		-4.06×10^{-4} (-1.00×10^{-3} – (-3.02×10^{-5})
Inter-individual variability			
CL_{Cap}/F [%]	40.1 (26.4)	5.3	39.2 (13.9 – 91.9)
V_{Cap}/F [%]	39.7 (36.7)	20.6	43.9 (12.0 – 110)
CL_{DFCR}/F [%]	32.2 (25.5)	3.2	32.6 (3.83 – 63.2)
V_{DFCR}/F [%]	47.6 (35.5)	13.4	50.1 (19.2 – 96.3)
$k_{e,\ DFUR}$ [%]	29.3 (25.9)	4.6	27.5 (16.7 – 40.6)
Residual variability			
Capecitabine [%]	60.1 (10.9)	3.9	58.8 (43.4 – 77.5)
DFCR [%]	46.1 (8.1)	4.7	45.1 (34.2 – 56.2)
DFUR [%]	45.2 (7.8)	4.7	42.9 (32.2 – 52.4)

CL_{Cap}/F, CL_{DFCR}/F: apparent capecitabine/DFCR clearance, V(Cap)/F, V(DFCR)/F: apparent capecitabine/DFCR volume of distribution, $k_{e,\ DFUR}$: elimination rate constant for DFUR, k_a: first-order absorption rate constant

Tab. 3 Parameter estimates of the regorafenib-metabolite model

Parameter	Estimate (relative standard error, %)	Shrinkage [%]	Bootstrap median (95% confidence intervals)
$CL_{Regorafenib}/F$ [L/h]	1.94 (12.1)		1.91 (1.47 – 2.46)
V_c/F [L]	10.4 (33.2)		9.83 (2.37 – 23.2)
$MAT_{Regorafenib}$ [h]	3.01 (9.6)		3.05 (2.03 – 4.05)
V_p/F [L]	63.9 (8.7)		64.4 (50.3 – 85.2)
Q/F [L/h]	13.5 (10.8)		13.7 (9.64 – 17.7)
CL_{M-2}/F [L/h]	0.936 (10.8)		0.932 (0.731 – 1.19)
$k_{g,met}$ [1/h]	0.265 (12.8)		0.267 (0.168 – 0.449)
MAT_{M-2} [h]	1.90 (14.1)		1.91 (1.31 – 2.96)
CL_{M-5}/F [L/h]	2.01 (21.7)		2.02 (1.14 – 3.16)
Inter-individual variability			
$CL_{Regorafenib}/F$ [%]	38.1 (23.6)	3.1	34.5 (14.8 – 48.0)
V_c/F [%]	131.5 (24.2)	3.7	126.9 (82.3 – 238.7)
MAT (Regorafenib) [%]	21.7 (24.7)	4.4	19.9 (5.92 – 30.0)
CL_{M-2}/F [%]	25.2 (33.6)	11.6	23.7 (6.15 – 37.9)
CL_{M-5}/F [%]	75.6 (22.3)	0.1	72.6 (50.1 – 99.3)
Residual variability			
Regorafenib [%]	52.6 (7.4)	3.6	51.2 (42.5 – 59.0)
M-2 [%]	57.9 (8.1)	1.5	57.9 (52.2 – 63.6)
M-5 [%]	54.1 (9.1)	4.7	53.6 (48.1 – 59.4)

$CL_{Regorafenib}/F$, CL_{M-2}/F, CL_{M-5}/F: apparent regorafenib/M-2/M-5 clearance, V_c/F: apparent shared central volume of distribution, V_p/F: apparent shared peripheral volume of distribution, Q/F: apparent shared intercompartmental clearance, $MAT_{Regorafenib}/MAT_{M-2}$: mean absorption time of regorafenib/M-2 defined as *n* transit compartments/transit constant k_{tr}, $k_{g,\,met}$: presystemic metabolic rate constant

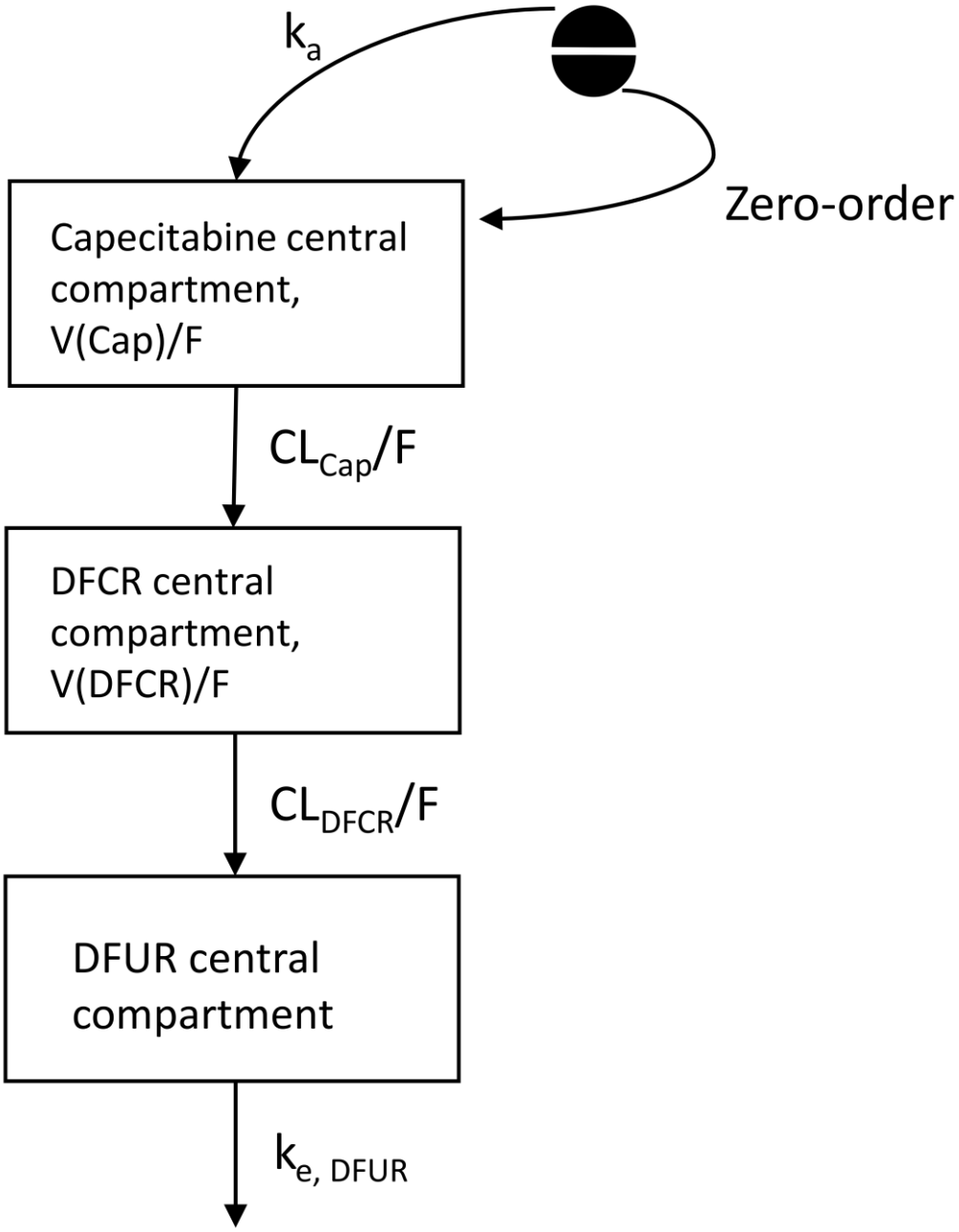

Fig. 1 Model structure of the capecitabine-metabolite model. DCFR: 5'-deoxy-5-fluorocytidine, DFUR: 5'-deoxy-5-fluorouridine, CL_{Cap}/F, CL_{DFCR}/F: apparent capecitabine/DFCR clearance, V(Cap)/F, V(DFCR)/F: apparent capecitabine/DFCR volume of distribution, $k_{e,\ DFUR}$: elimination rate constant for DFUR, k_a: first-order absorption rate constant.

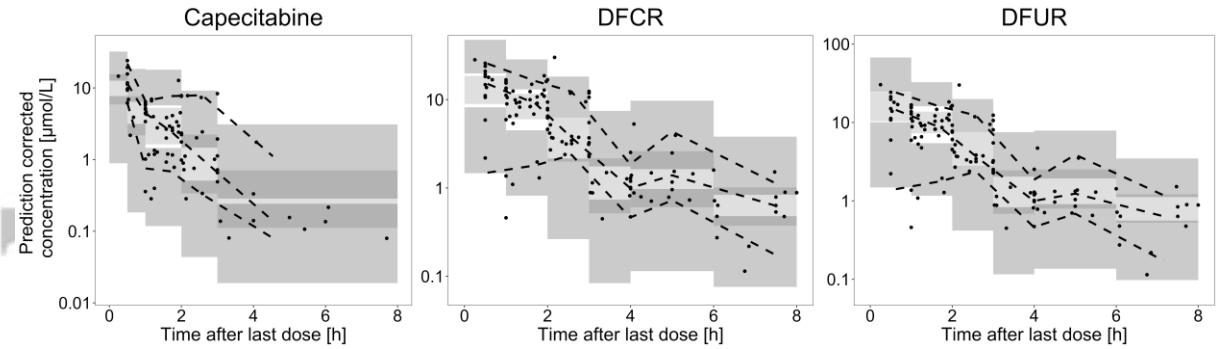

Fig. 2 Prediction-corrected visual predictive checks of capecitabine, DFCR and DFUR. Black dots: Prediction-corrected observations, dashed lines: 90% interval and median of the prediction-corrected observations, dark grey shaded area: 95% confidence intervals of the 5th and 95th prediction interval, light grey shaded area: 95% confidence interval of median prediction.

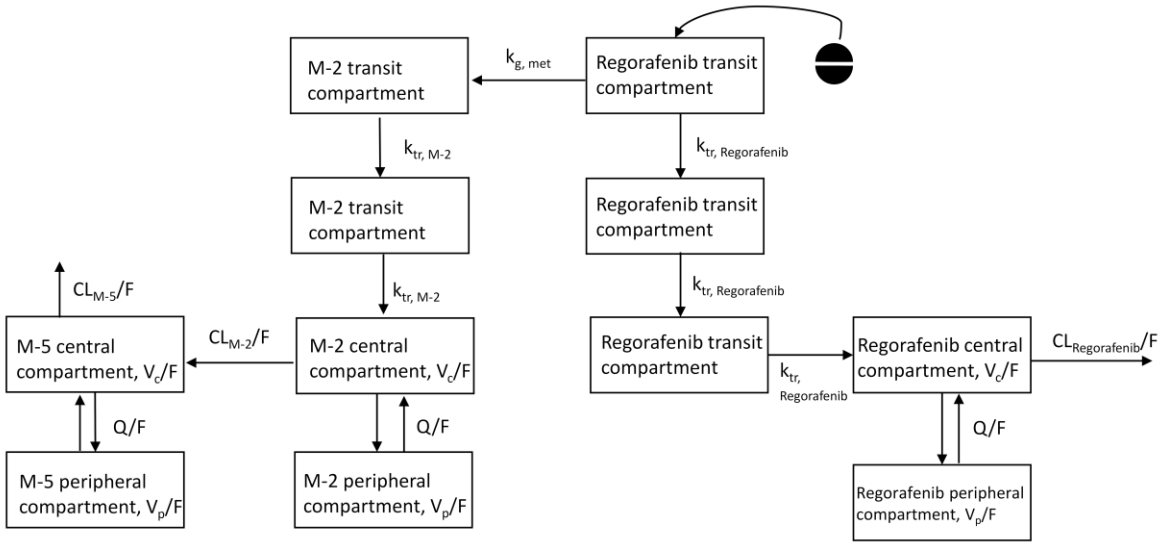

Fig. 3 Model structure of the regorafenib-metabolite model. $CL_{Regorafenib}/F$, CL_{M-2}/F, CL_{M-5}/F: apparent regorafenib/M-2/M-5 clearance, V_c/F: apparent shared central volume of distribution, V_p/F: apparent shared peripheral volume of distribution, Q/F: apparent shared intercompartmental clearance, $k_{tr, Regorafenib}/k_{tr, M-2}$: transfer rate constants defined as *n* transit compartments/mean absorption time, $k_{g, met}$: presystemic metabolic rate constant

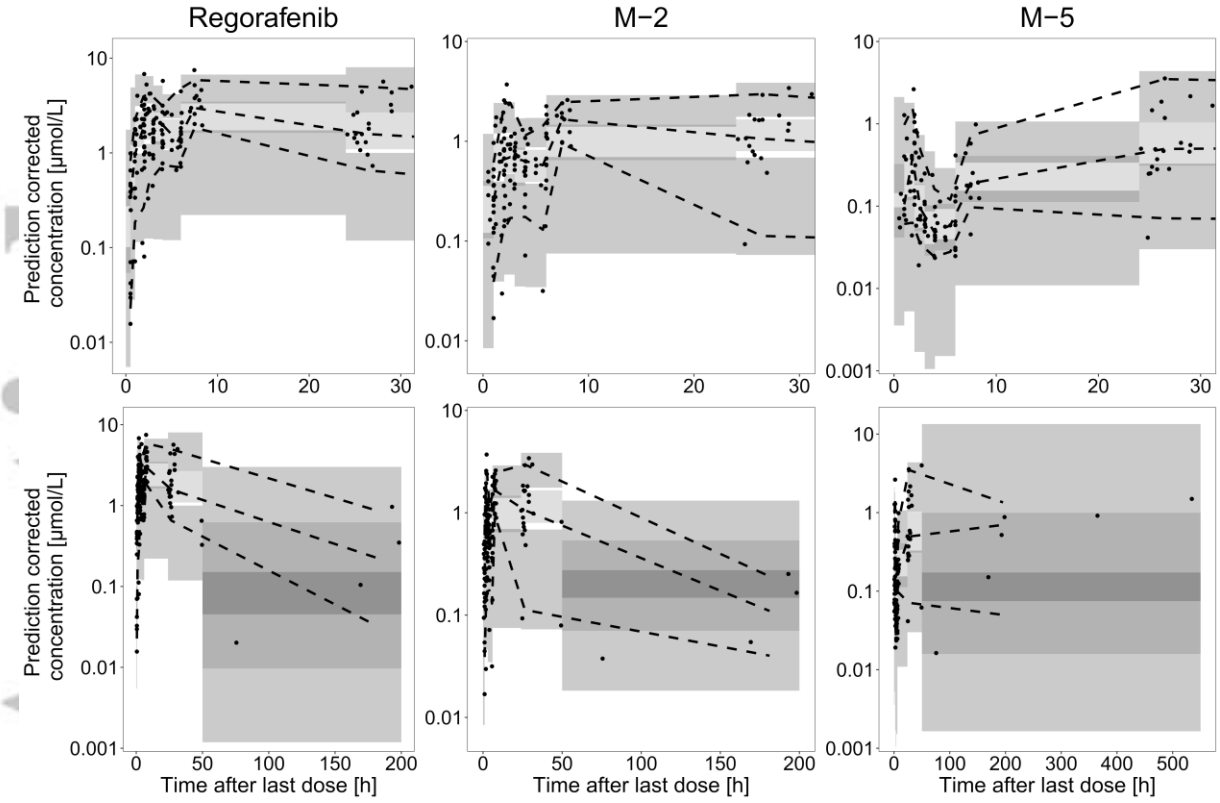

Fig. 4 Prediction-corrected visual predictive checks of regorafenib, M-2 and M-5 from 0 to 30 hours (upper panel) and from 0 to 200 hours (regorafenib, M-2, lower panel) as well as from 0 to 550 hours (M-5, lower panel). Black dots: Prediction-corrected observations, dashed lines: 90% interval and median of the prediction-corrected observations, dark grey shaded area: 95% confidence intervals of the 5th and 95th prediction interval, light grey shaded area: 95% confidence interval of the median prediction.

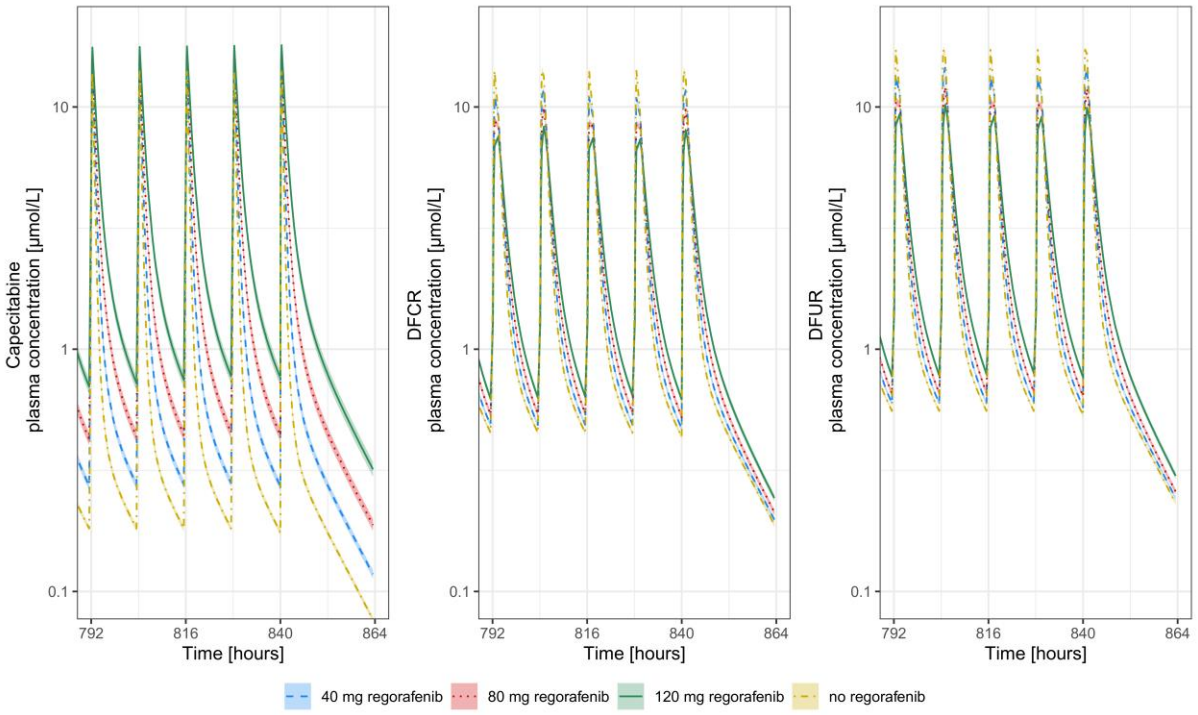

Fig. 5 Simulated plasma concentrations of capecitabine, DFCR and DFUR depending on regorafenib dosage from 792 – 864 hours.